Supporting Material for:

Molecular Mechanisms of HipA Mediated Multidrug Tolerance and its Neutralization by HipB

Maria A. Schumacher*, Kevin M. Piro, Weijun Xu, Sonja Hansen, Kim Lewis, and Richard G. Brennan*

*To whom correspondence should be addressed. E-mail: rgbrenna@mdanderson.org or maschuma@mdanderson.org

This supplement includes:

Materials and Methods
Table S1
Figs. S1 to S4

Supporting Information:

Materials and Methods

Crystallization of apoHipA and the HipA-ATP complex

To obtain milligram quantities of pure HipA, a HipA D309Q substitution was made that can be expressed in *E. coli* in the absence of HipB without leading to cell stasis (*15*). The mutant was subcloned into pBAD33 and the construct transformed into DH5α cells. The cloning placed a hexa-histidine tag plus serine and arginine immediately after the initiator methionine at the HipA N terminus. For overexpression, *E. coli* cells were inoculated with an overnight culture using chloramphenicol selection. Cells were grown at 37 °C to an OD_{600} of 0.5-0.6 and induced with arabinose for 2.5 hrs. After pelleting, the cells were lysed using a French Press and the supernatant loaded onto a Ni-NTA column. The protein was purified using a 10-500 mM imidazole gradient. Purified fractions were pooled and concentrated for crystallization. ApoHipA crystals were grown at room temperature via hanging drop, vapor diffusion methods using a reservoir of 16% PEG 8000, 20% glycerol and 0.04 M potassium phosphate, pH 7.5. The crystals grow over a period of a week and diffract to beyond 1.6 Å resolution. The crystals take the monoclinic space group $P2_1$ with a = 48.7 Å, b = 85.8 Å, c = 49.7 Å and β = 90.1°. For cryoprotection, apoHipA crystals were taken straight from the drop and frozen in the cryostream. Intensity data were processed with MOSFLM. Crystals of the HipA-ATP complex were obtained by mixing the purified protein containing 1 mM ATP and 5 mM $MgCl_2$ with a reservoir of 30% PEG 600, 0.1 M CHES pH 9.5. The HipA-ATP complex crystallized nonisomorphously with respect to the apo form of HipA and takes the monoclinic crystal form, space group $P2_1$ with a = 68.5 Å, b = 84.1 Å, c = 69.3 Å and β = 91.5°. For cryoprotection, HipA-ATP crystals were dipped for several minutes in the crystallization solution plus 30% glycerol. Intensity data were processed with MOSFLM.

Structure determinations of apoHipA and the HipA-ATP complex

To determine the HipA structures, selenomethionine-substituted HipA was produced using the methionine inhibitory pathway. The protein was crystallized using conditions for obtaining apo and ATP-bound HipA. Three wavelength MAD data sets were collected for selenomethionine-substituted apoHipA and HipA-ATP crystals. The data were processed with MOSFLM and the

selenium sites were located using SOLVE (*16*). The MAD maps were of excellent quality and allowed complete tracing of the HipA structure using O (Fig. S1) (*18)*. Model building was carried out using O and refinement with CNS (*17-18*). The final apoHipA structure, which contains one molecule per asymmetric unit (ASU), includes residues 2-109, 114-134, 146-184, 196-437, 1 chloride ion, 1 phosphate ion and 377 water molecules and has R_{work}/R_{free} values of 19.5%/23.2%. The final HipA-ATP structure, which contains two molecules of HipA-ATP in the ASU, includes residues 2-105, 114-184, 196-437 of one molecule, residues 3-183, 198-435 of the other molecule, 2 ATP molecules, 4 Mg^{2+} ions, 2 CAPS sulphate groups and 868 water molecules and has R_{work}/R_{free} values of 18.4%/21.7%. The two HipA-ATP molecules in the ASU are essentially identical as their Cα atoms can be superimposed with an RMSD of 0.30 Å. Both the apoHipA and HipA-ATP structures have excellent geometry as ascertained by Ramachandran analyses (Table S1).

Crystallization of the HipA-HipB-DNA complex

An artificial *hipB* gene was designed and purchased from Genscript Corporation, Piscatway, NJ, USA; Web:www.genscript.com. This gene was codon optimized for protein expression in *E. coli* and subcloned into the pET15b vector such that the N-terminal hexa-histidine tag was expressed for purification via Ni-NTA column chromatography. The expression vector was transformed into competent BL21(DE3) cells. The protein was expressed by the addition of 1.0 mM IPTG for 3 hrs at 20 °C. To form the HipA-HipB complex the two purified proteins were mixed stoichiometrically, ~1:1 (1 HipB dimer:2 HipA molecules) in Buffer A (25 mM Tris pH 7.5, 100 mM NaCl, 1 mM DTT, 5% glycerol). The complex was further purified by S200 size exclusion chromatography and concentrated to 10 mg/mL for crystallization. To obtain crystals of the HipA-HipB-DNA complex, several oligodeoxynucleotides (Oligos Etc., Wilsonville, OR), each of which encompassed the 20 bp *hipB* operator, were mixed in a ratio of 1 DNA duplex to (1 HipB dimer:2 HipA molecules) and used in crystallization screens. Data quality crystals were obtained with a 21 mer DNA site, which has 5´ adenosine overhangs. To grow the crystals, the HipA-HipB-DNA solution was mixed 1:1 with a reservoir of 0.5% PEG 5000, 0.8 M potassium/sodium tartrate tetrahydrate and suspended over the same reservoir. Crystals took several weeks to grow and diffracted anisotropically to a limiting resolution of 2.5 Å in the best

direction and 3.3 Å in the worst direction. Crystals were cryopreserved by dipping for several minutes in saturated lithium sulphate and annealling. All data were processed with MOSFLM.

Structure determinations of HipA-HipB-DNA and HipA(ATP)-HipB-DNA complexes

The structure of the HipA-HipB-DNA complex was solved by Molecular Replacement using MolRep and the HipA (either apo or ATP bound) structure as a search model. The crystals contain one HipA monomer, one HipB subunit and one DNA half site in the ASU with crystallographic symmetry generating the dimeric complex. After initial refinement, difference Fourier electron density maps revealed clear density for HipB and the DNA, which were built using O (*18*). The final structure includes HipA residues 2-184, 196-437; HipB residues 4-74, all nucleotides of the DNA, 8 sulphate ions and 34 water molecules. HipB has topology α1–α2–α3–α4–β1 (α1;residues 10-24, α2; 28-35, α3; 39-48, α4; 54-65, β1; 66-72). To obtain the structure of the HipA(ATP)-HipB-DNA complex, ATP and $MgCl_2$ were added to final concentrations of 5 mM each to purified HipA-HipB solutions, which were then mixed with DNA in the same stoichiometry used to obtain HipA-HipB-DNA crystals. This *de novo* crystallization was carried out as per the HipA-HipB-DNA complex and isomorphous tetragonal crystals were obtained. Data collected on such crystals revealed clear density for ATP. Data were also collected for HipA-HipB-DNA crystals soaked with 5 mM ATP and 5 mM $MgCl_2$ for several days to 1 week. The crystals were cryoprotected as for the HipA-HipB-DNA complex using lithium sulphate, however 5 mM ATP and 5 mM $MgCl_2$ were added to the cryoprotectant. Intensity data were collected at ALS Beamline 8.2.1 and processed with MOSFLM. Structures were solved by Molecular Replacement using the HipA-HipB-DNA complex as a search model. Clear density was observed for the ATP molecule in both ATP co-crystallized and soaked crystals after initial rounds of refinement. The best data was obtained for a soaked crystal (to 2.98 Å resolution compared to 3.2 Å resolution for the *de novo* crystallized complex) and the final R_{factor}/R_{free} for this structure is 26.2%/28.2 % to 2.98 Å resolution. The final structure includes HipA residues 2-184, 196-437; HipB residues 4-74, all nucleotides of the DNA, 1 ATP molecule, 9 sulphate ions and 4 water molecules.

Binding affinity of ATP for HipA and the HipA-HipB complex

The binding affinities of HipA and HipA-HipB for ATP were determined by isothermal titration calorimetry (ITC). All protein samples were dialyzed extensively into Buffer B (25 mM Tris pH 7.5, 300 mM NaCl, 5% glycerol and 5 mM $MgCl_2$) while ATP was directly dissolved into this dialysis buffer. Prior to dialysis, the HipA-HipB complex was purified further via S200 size exclusion chromatography in order to ensure isolation of stoichiometrically bound HipA-HipB complex. Protein concentrations were measured by Bradford Assay (Biorad). Immediately prior to the ITC experiment, samples were degassed. ATP (3 mM) was titrated into 110 μM protein and the change in heat was monitored using a VP-ITC instrument (MicroCal, Inc.). Additional control experiments, in which 3 mM ATP was titrated into dialysis buffer alone and dialysis buffer was titrated into 110 μM HipA, yielded negligible heats of dilution. Thermogram analysis was performed using the Origin 5.0 package.

Candidate HipA substrate pulldowns

Candidate *E. coli* proteins included tryptophanase and EF-Tu. Tryptophanase has been implicated in biofilm formation and EF-Tu was known to be phosphorylated on Thr^{382} by an unknown kinase(s). Moreover, eukaryotic Ser/Thr kinases have been shown to be capable of phosphorylating *E. coli* EF-Tu residue Thr^{382} (*23*). Thus, both were deemed possible candidate substrates for HipA. Candidate proteins, which contained either GST affinity tags (EF-Tu) or no tags (tryptophanase) were incubated with purified His-tagged HipA D309Q for 30 min at room temperature and then either pulled down with glutathione agarose or Ni-NTA resin and washed with 25 mM Tris, pH 7.5, 100 mM NaCl, 5% glycerol before elution with either glutathione or imidazole. The pulldowned proteins were resolved by SDS PAGE and visualized by Coomassie brilliant blue. HipA alone was not retained on glutathione agarose beads (in the presence or absence of ATP and/or GDP) and was found in the eluate even without the wash step indicating that it has neglible affinity for glutathione agarose. To assess tryptophanase binding to HipA, HipA was bound to Ni-NTA and a lysate from cells containing induced, non-tagged tryptophanase was added, mixed for several hrs and eluted. From these studies, no binding between HipA and tryptophanase was observed. To examine EF-Tu binding to HipA, GST pulldowns were performed. GST-fused EF-Tu was adsorbed to glutathione agarose and HipA added, mixed and eluted. HipA was retained in samples containing ATP and GDP (Fig. 1D).

in vitro translation of wild type HipA

Wild type (wt) HipA cannot be produced in *E. coli* due to its inhibition of cell growth. Thus, to produce wt HipA protein, a wheat germ *in vitro* transcription/translation system was used (Roche Diagnotics, Switzerland). The *hipA* gene, including sequences encoding the N-terminal hexa-histidine tag, was inserted into the pIVEX 1.3 WG vector between the NdeI and XmaI sites. Subsequently, 2 μg of recombinant DNA were added to 50 μL of the translation reaction, which was reconstituted as specified by the Roche manual (Germ CECF Kit (Roche Diagnostics)). Reactions were run at 24 °C with continuous shaking for 24 hrs. To purify wt HipA protein, a Ni-NTA batch purification was carried out. Reaction lysate was equilibrated with Ni-NTA resin (8:1 lysate volume to resin bed volume ratio) in a 1.5 mL Eppendorf microtube for 30 min on an orbital shaker, and the supernatant was then separated from the resin by centrifugation. Resin was washed with a total volume of 4 mL of Buffer B in increments of 0.75 mL. wt HipA was eluted with Buffer B plus 500 mM imidazole. Samples were run on an SDS gel to analyze purity, which ranged between 60-70%. Western blot analysis was done using an anti-His antibody to confirm that the protein, which migrated at a molecular weight of ~50 kDa, was His-tagged wt HipA (fig. S3).

EF-Tu phosphorylation by HipA

The partially purified, *in vitro* translated wt HipA protein was used in EF-Tu phosphorylation assays. 30 μL reactions were run in a solution of 20 mM Tris, pH 7.5, 100 mM NaCl, and 10 mM $MgCl_2$. Either wt HipA or HipA D309Q was added to an aliquot of EF-Tu (either GST-EF-Tu or factor X_a cleaved EF-Tu, which no longer contains the GST tag) with and without relevant nucleotide substrates. To test the effect of the wheat germ cell extract on the phosphorylation assay, a control vector was subjected to the same conditions as the *hipA* recombinant DNA and the product was then combined with EF-Tu. Each reaction contained 20 mM ATP. The reactions were incubated at room temperature for 1 hr and stopped by the addition of 15 μL 2X SDS-PAGE loading buffer and heated at 95 °C for 5 min. To assay for phosphorylation, an ImmunoBlot analysis was done. Samples were run on Tris-HCl SDS-PAGE 10-20% gradient gels (Biorad), transferred to PVDF membranes, and blocked with 2% BSA in 1X phosphate buffered saline (PBS), 0.2% Tween-20 (PBST) for two hrs. The membranes were

immunoblotted with primary antibodies specific for phosphoserine/phosphothreonine/phosphotyrosine residues (AnaSpec, San Jose, CA) followed by incubation for two hrs. with horseradish peroxidase-conjugated anti-mouse secondary antibodies, both in 2% BSA, 1X PBST. The blot was visualized by chemiluminescense using an Alpha Imager (Alpha Innotech, San Leandro, CA).

Fluorescence polarization (FP) binding of EF-Tu peptide by HipA

FP binding studies were carried out with an N-terminal-fluorescein labelled peptide, IREGGR**T**VGA, where the position of EF-Tu Thr^{382} is bolded. The measurements were made using a PanVera Beacon 2000 Fluorescence Polarization System equipped with 490 nM excitation filters and 530 nM emission filters. Binding studies are carried out by titrating the D309Q protein (using typical protein concentrations of 10 μM - 250 μM) into 0.500 mL binding buffer (25 mM Tris pH 7.5, 300 mM NaCl, 5% glycerol, 1 mM ATP, 1 mM $MgCl_2$) containing 1 nM fluoresceinated peptide. The resulting binding isotherm was plotted by fitting to a simple bimolecular binding model using nonlinear regression. The K_d was 15 ± 5 μM for HipA binding to the EF-Tu peptide. As a control, another 10-mer peptide with the sequence ESTEQQNLEW was used for FP measurements under the identical conditions and revealed no saturable binding up to final HipA concentrations of 300 μM at which point the protein started to precipitate.

Crystallization and structure determination of HipA-(AMP-PNP)-EF-Tu peptide complex

To obtain crystals of the HipA-(AMP-PNP)-EF-Tu peptide complex, HipA at 5 mg/mL was mixed with 1 mM AMP-PNP, 1 mM $MgCl_2$ and the peptide, IREGGRTVGA, was added in saturating amounts to the solution. The complex was mixed 1:1 with a reservoir of 1 M sodium acetate trihydrate and sealed over a dry reservoir. Crystals grew in 2-3 days and could be cryopreserved directly from the drop. Data were collected on an R-Axis-HTC and processed with CrystalClear. The crystals are tetragonal, I422, with a = b = 128.4 Å and c = 203.9 Å. Crystals typically diffract to 5.0 Å resolution. However, one crystal diffracted to 3.5 Å resolution and was collected for structure determination. The intensity data have an overall I/σI of 7.3 and 2.3 for the highest resolution shell. The R_{symm} for all the data is 12.4% and 39.0% for the highest resolution shell. The structure was solved by Molecular Replacement using MolRep and the HipA-ATP structure as a search model. The crystals contain one HipA monomer in the ASU.

After initial refinement, difference Fourier electron density maps revealed clear density for the AMP-PNP and activation loop residues 185-195, which were missing in all previous structures. After several round of positional refinement, contiguous density was observed near the active site, which could be fit with the peptide. However, because of the limited resolution the peptide was as built as a polyalanine chain. The final structure includes HipA residues 2-437, the AMP-PNP molecule and 9 peptide residue built as a polyalanine chain. The structure has an R_{work}/R_{free} of 29.1%/36.0% with excellent geometry.

Table S1: Selected crystallographic data for HipA and HipA-HipB-DNA complexes

Crystal	apoHipA	HipA-(ATP)	HipA-HipB-DNA	HipA(ATP)-HipB-DNA
Space group	$P2_1$	$P2_1$	P422	P422
Cell dimensions	a=48.7 Å	a=68.5 Å	a=166.3 Å	a=167.2 Å
	b=85.8 Å	b=84.1 Å	b=166.3Å	b=167.2 Å
	c=49.7Å	c=69.3 Å	c=62.1 Å	c=62.4 Å
	β=90.1°	β=91.5		
Molecules/ASU (#)	1	2	1	1
Beamline	8.2.1 (ALS)	8.3.1 (ALS)	8.3.1 (ALS)	8.2.1 (ALS)
Resolution (Å)	43.03-1.54	42.64-1.66	74.33-2.68	118.70-2.98
Overall R_{sym}(%)[a]	5.4 (38.7)[b]	5.4 (29.5)	7.1 (38.3)	7.8 (43.4)
Overall I/σ(I)	13.7 (2.0)	10.5 (3.2)	9.0 (2.0)	7.3 (1.9)
Total Reflections (#)	164732	361604	149024	64025
Unique Reflections (#)	59003	89054	25017	18730
Completeness (%)	98.1 (97.3)	96.3 (94.2)	99.7 (99.3)	99.6 (99.7)
Refinement Statistics				
Resolution (Å)	43.03-1.54	42.64-1.66	74.33-2.68	118.7-2.98
R_{work}/R_{free}(%)[c]	19.5/23.2	18.4/21.7	22.5/28.1	26.2/28.2
Rmsd				
Bond angles (°)	1.63	1.44	1.20	1.55
Bond lengths (Å)	0.013	0.010	0.007	0.012
B factors (Å^2)	2.4	1.8	2.8	4.3
Ramachandran analysis				
Most favored (%/#)	93.8/334	92.9/677	88.0/375	85.1/368
Add. allowed (%/#)	6.2/22	6.7/49	11.0/47	14.5/63
Gen. allowed (%/#)	0/0	0.3/2	0.9/4	0.5/2
Disallowed (%/#)	0/0	0.1/1	0/0	0/0

[a] $R_{sym} = \Sigma\Sigma|Ihkl-Ihkl(j)|/ \Sigma Ihkl$, where Ihkl(j) is observed intensity and Ihkl is the final average value of intensity.

[b] values in parentheses are for the highest resolution shell.

[c] $R_{work} = \Sigma||F_{obs}| - |F_{calc}||/\Sigma|F_{obs}|$ and $R_{free} = \Sigma||F_{obs}| - |F_{calc}||/\Sigma|F_{obs}|$; where all reflections belong to a test set of 5% randomly selected data.

Figure S1.

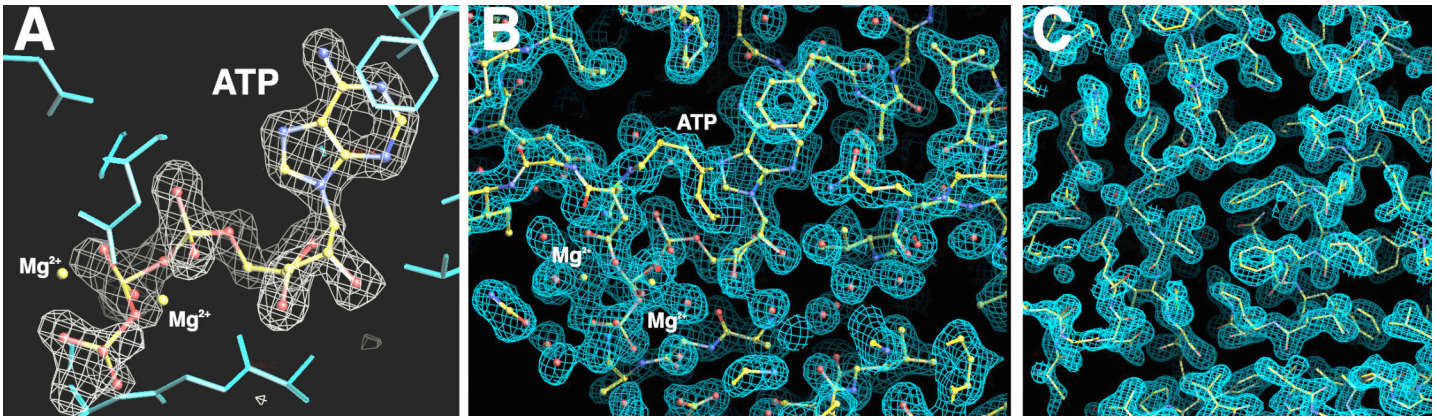

Figure S1. HipA binds ATP-Mg^{2+}.
(A) Omit F_o-F_c map contoured at 4.5 σ and calculated to 1.66 Å resolution in which the ATP molecules were omitted from the HipA-ATP structure. HipA side chains are colored cyan and shown as sticks. The ATP molecule is shown as sticks with carbon, nitrogen, oxygen and phosphorus atoms colored yellow, blue, red and dark yellow, respectively. The electron density map is shown as a grey mesh. The Mg^{2+} ions, which were not omitted, and the ATP are labeled.
(B) Experimental MAD map of the HipA-ATP structure contoured at 1.7 σ and calculated to 1.70 Å resolution. The electron density map is shown as a blue mesh and the side chains are shown as sticks with carbon, nitrogen, oxygen and phosphorus atoms colored yellow, blue, red and dark yellow, respectively. This figure shows a view centered on the ATP binding site.
(C) A different section of the experimental MAD map shown in B. The contour level is 1.7 σ and the map was calculated to 1.70 Å resolution. These Figures were made using O (*18*).

Figure S2.

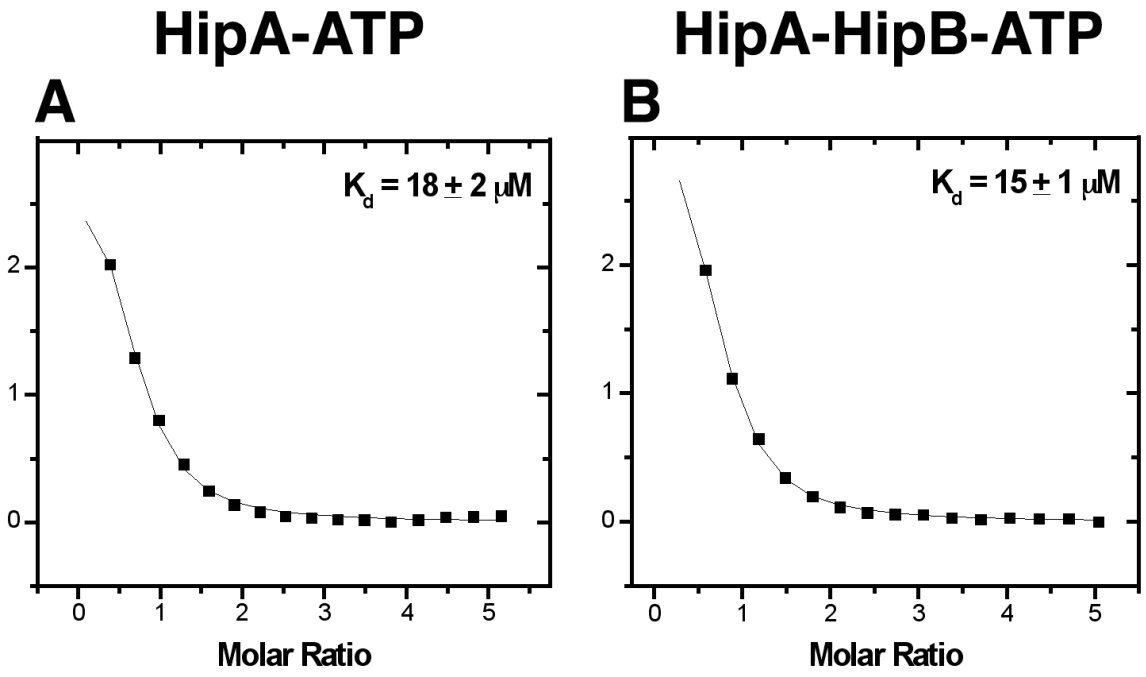

Figure S2. Isothermal titration calorimetry fitted thermograms of ATP binding to HipA (**A**) and to HipA in the HipA-HipB complex (**B**). The integrated binding isotherms are corrected for ligand and protein dilution effects. The integrated binding isotherms show essentially identical curves indicating that the HipA interaction with HipB does not obstruct or change the ability of HipA to bind ATP.

Figure S3.

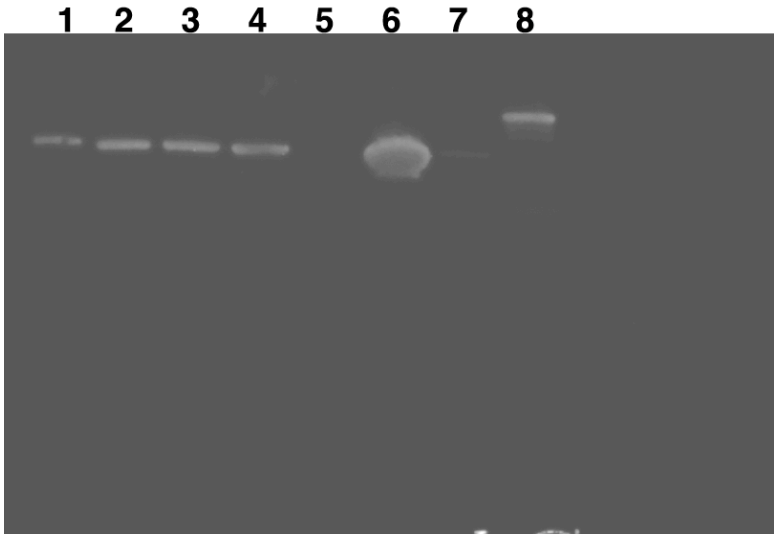

Figure S3. Immunoblot of *in vitro* transcription/translation experiments used to obtain wild type HipA. HipA contains an N-terminal hexa-histidine tag and was purified by Ni-NTA chromatography. The presence of the protein was probed with an anti-his-tag antibody and visualized by chemiluminescence exposure with an Alpha Inotech. The presence of the wild type protein was confirmed by this blot. The lanes correspond to the following:

1. 2 μL of purified wt HipA
2. 4 μL of purified wt HipA
3. 6 μL of purified wt HipA
4. 8 μL of purified wt HipA
5. MW Ladder (no his-tagged proteins)
6. 1 μL of hexa-histidine tagged D309Q produced from *E. coli*
7. 2 μL of Ni-NTA wash, before elution of wt HipA from Ni-NTA column
8. GUS Control Reaction (positive control, β-glucuronidase with His-tag)

Figure S4.

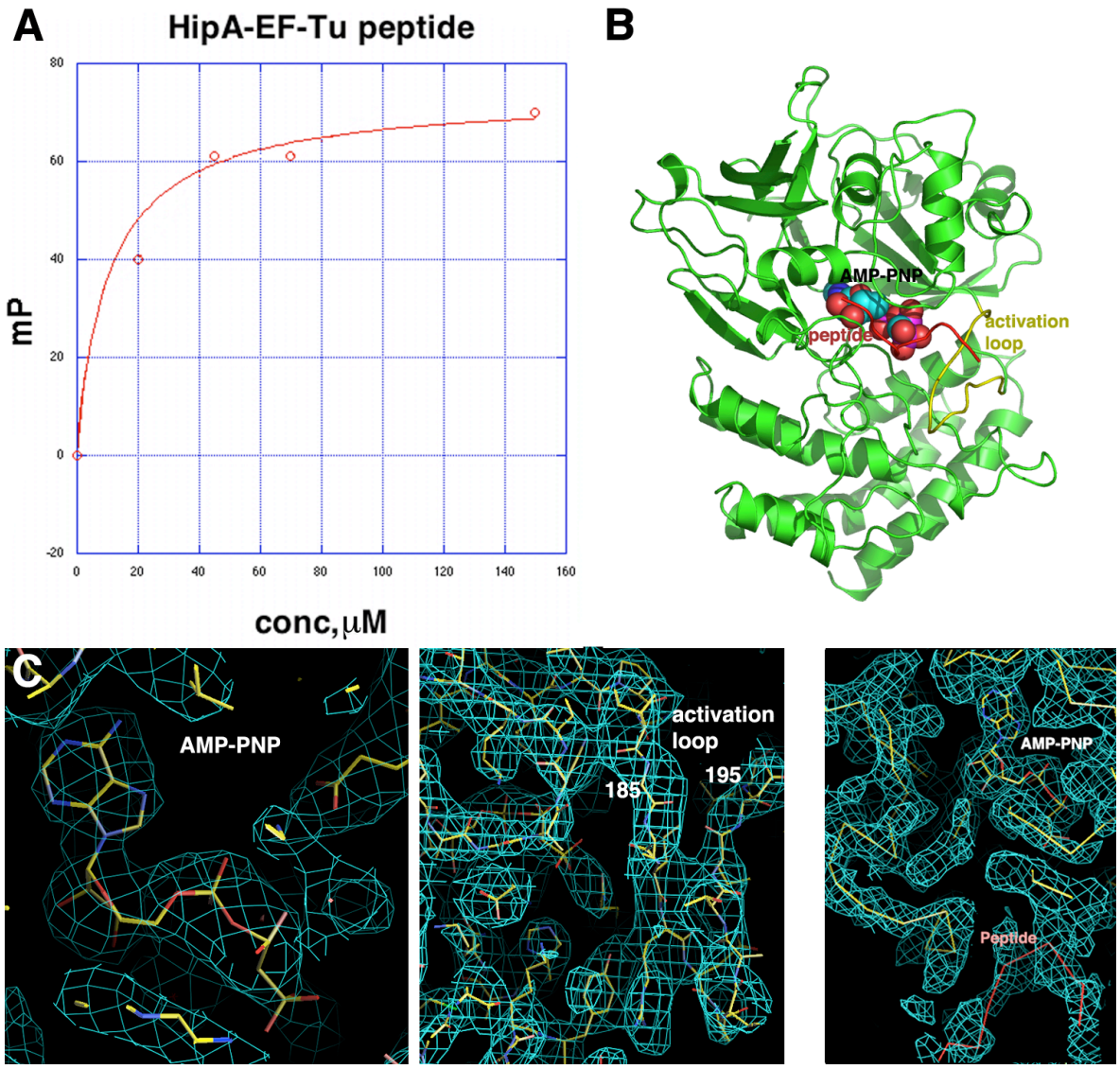

Figure S4. **(A)** Representative fluorescence polarization binding isotherm of the HipA EF-Tu peptide, IREGGRTVGA, interaction. A K_d of 15 ± 5 μM was obtained. (**B**) Ribbon diagram of the HipA-(AMP-PNP)-EF-Tu peptide structure solved to 3.5 Å resolution. The activation loop, which is only observed in the structure with the peptide, is colored yellow and the peptide is

colored red. The AMP-PNP molecule is shown as CPK. (**C**) Views of the $2F_o$-F_c map of the HipA-(AMP-PNP)-peptide structure contoured at 0.9 σ. (Left) Close up view of the AMP-PNP molecule. (Middle) View of the excellent density for activation loop (residues 185-195), which is continuous. (Right) views of the electron density of the peptide (red Cα trace). Density for the peptide was strongest near the active site pocket, but side chains were not clearly discernable and therefore the peptide was built as a polyalanine chain.